Doubly Temperature Sensitive Core−Shell Microgels

Ingo Berndt and Walter Richtering*

Institut für Physikalische Chemie, Christian-Albrechts-Universität zu Kiel, Olshausenstrasse 40, D-24098 Kiel, Germany

Received June 6, 2003; Revised Manuscript Received September 2, 2003

ABSTRACT: We report on synthesis and characterization of doubly temperature sensitive core−shell microgels. These core−shell microgels are composed of a core of chemically cross-linked poly(*N*-isopropylacrylamide) (PNIPAM) and a shell of cross-linked poly(*N*-isopropylmethacrylamide) (PNIPMAM). PNIPAM exhibits in water a lower critical solution temperature (LCST) of ca. 34 °C, and the LCST of PNIPMAM is ca. 45 °C. Solution properties were investigated by means of dynamic light scattering (DLS), optical transmission, differential scanning calorimetry (DSC), and small-angle neutron scattering (SANS). Core−shell microgels of this composition display a temperature-dependent two-step shrinking behavior. The influences of the content of the cross-linking agent *N*,*N*′-methylenbis(acrylamide) (BIS) and of the thickness of the PNIPMAM shell on the thermosensitive response of the PNIPAM/PNIPMAM core−shell microgels were investigated. Core−shell microgels with a thick shell do not show a size transition at the PNIPAM LCST anymore. The volume transition is adjustable by varying the cross-link density of the shell. The swelling behavior of the core−shell microgels is compared to that of pure PNIPAM and PNIPMAM. Additionally, an inverse system consisting of a PNIPMAM core and a PNIPAM shell was prepared and investigated by DLS. Here the collapsed shell at intermediate temperatures strongly restricts the core swelling so that the overall size of the core−shell microgel is smaller as compared to the pure core.

Introduction

Environmentally sensitive microgels attract attention because of their versatility to many fields as, e.g., drug delivery[1], catalysts,[2] and chemical separation. The probably most studied responsive polymer is cross-linked poly(*N*-isopropylacrylamide) (PNIPAM).[3−5]

Aqueous PNIPAM solutions display phase separation upon heating with a lower critical solution temperature LCST of ca. 34 °C. Microgels are internally cross-linked spherical particles swollen by the solvent with a typical size in the range 50−1000 nm. PNIPAM microgels shrink upon heating with a sharp transition a the LCST. Since monodisperse PNIPAM microgels are readily accessible via emulsion polymerization, they can be considered as model systems for colloid science,[6] and the influence of various parameters, e.g., cross-link density,[7] comonomers,[8,9] solvent composition,[10] salt effects,[11] etc., on the particles' properties has been investigated.

Recently Lyon and co-workers demonstrated that the versatility can be enhanced when core−shell microgels with different properties of core and shell are prepared.[12−14] They synthesized PNIPAM core−shell microgels where either core or shell consisted of a copolymer of PNIPAM with acrylic acid (AAc). Incorporation of AAc shifts the LCST to higher temperatures and furthermore introduces a pH sensitivity. These core−shell microgels are multiresponsive.

In this contribution we report on a different approach, namely the preparation of core−shell microgels based on PNIPAM as core and poly(*N*-isopropylmethacrylamide) (PNIPMAM) as shell polymer, the LCST of which is ca. 45 °C. An inverse system with a PNIPMAM core and a PNIPAM shell was also prepared, which exhibits interesting features. Pure PNIPMAM microgels behave similarly to PNIPAM microgels. The influence of cross-link density on the thermosensitivity of PNIPMAM was investigated in detail by Duracher and coworkers.[15,16]

The enhanced variety of material properties enables advances in pharmaceutical and cosmetical application, filters, and protein immobilization. The objective of our study was to explore the possibility to control the temperature-dependent size and colloidal stability of core−shell microgels via the variation of thickness and cross-link density of the PNIPMAM shell.

Experimental Section

Materials. NIPAM and NIPMAM monomers and BIS were purchased from Aldrich. NIPMAM monomer was recrystallized from cyclohexane. Sodium dodecyl sulfate (SDS) and the initiator potassium peroxodisulfate (KPS) were purchased from Merck Eurolab and used as received. Water for all purposes was ion-exchanged to a resistance of 18.2 MΩ/cm (Milli-Q) and filtered through a 0.2 μm filter.

PNIPAM Core Synthesis. PNIPAM core microgel particles were prepared via free radical emulsion polymerization as reported previously. Polymerization was performed in a 1 L reaction vessel equipped with a mechanical stirrer, reflux condenser, thermometer, and gas inlet. 11.80 g of NIPAM, 0.225 g of BIS, and 0.225 g of SDS were dissolved in 0.6 L of water at 70 °C and purged with nitrogen for at least 1 h. Polymerization was initiated with 0.45 g of KPS dissolved in 5 mL of water and carried out for 6 h under a nitrogen stream and constant stirring at 400 rpm. The dispersion was passed through glass wool in order to remove particulate matter and dialyzed against deionized water for 30 days to a conductance < 0.01 mS. For details see ref 6.

PNIPMAM Shell Synthesis. PNIPMAM shell synthesis was performed using core particles as nuclei for subsequent emulsion polymerization. A core solution was heated to 70 °C and purged with nitrogen. A separately prepared mixture of NIPMAM monomer, BIS, and SDS was added after 1 h, and the mixture was purged with nitrogen for 1 h. Shell polymerization was initiated with KPS solved in 5 mL of degassed water (for details see Table 1). The synthesis proceeded for 6

* To whom all correspondence should be addressed: e-mail richtering@phc.uni-kiel.de; Tel +49 431 880-2831; Fax +49 431 880-2830.

10.1021/ma034771+ CCC: $25.00
Published on Web 10/15/2003

Table 1. Experimental Conditions for Core−Shell Microgel Syntheses

	core solution	shell solution				
sample	PNIPAM [g/mL]	NIPMAM [g]	BIS [g]	KPS [g]	SDS [g]	water [mL]
CS005	0.0238	1.19	0.143	0.023	0.0103	50
CS006	0.0119	1.19	0.143	0.023	0.0103	50
CS008	0.0025	1.19	0.143	0.023	0.0103	50
CS009	0.0238	0.571	0.0686	0.0011	0.0048	30
CS010	0.0238	0.476	0.0303	0.0092	0.0040	25
CS011	0.0238	0.476	0.0178	0.0092	0.0041	25
INV001	0.0199 (PNIPMAM)	0.493 (NIPAM)	0.0353	0.0124	0.0052	25

h at constant stirring at 200 rpm. The product was passed through glass wool and dialyzed in the same way as the core particles.

Dynamic Light Scattering. Particle sizes were determined by dynamic light scattering (DLS). Light scattering experiments on the highly diluted samples (Milli-Q water) were carried out with an ALV goniometer equipped with an avalanche photodiode. The samples were allowed to equilibrate for 20 min at each temperature. Temperature programs have been run both directions, increasing and decreasing temperature. Temperature-dependent size changes are completely reversible, so only data of heating direction will be shown. Scattered light was detected at 90° with an integration time of 120 s and computed with a digital ALV 5000E autocorrelator using ALV Software version 5.3.2. Particle size were calculated by cumulant fits. The DLS data as well as the observation that the microgels form colloidal crystals at higher concentration reveal that the size polydispersity is less than 10%.

Optical Transmission. A Mettler Phototrode DP550 (λ = 550 nm) was used for transmission measurements on samples of ca. 0.5 wt %. Output voltage was received by a common multimeter (METEX 3640D) and transmitted to a personal computer. Transmission was measured at temperature increments of 0.5 °C with equilibration times of 2 min. Transmission data were normalized to initial transmission at T = 25 °C.

Small-Angle Neutron Scattering. SANS experiments were carried out at the Institut Laue-Langevin, Grenoble, France, on the D11 beamline. The data were collected using a two-dimensional detector with detector settings at 2, 10, and 36 m to cover a maximum q range of $0.002 < Å^{-1} < 0.15$ at 6 Å neutron wavelength. Data were background corrected and water normalized with ILL software GRASP.

Results

Two series of core−shell microgels were synthesized using the same PNIPAM microgel as core. One series of core−shell microgels with different PNIPMAM shell thickness was prepared. In the second series the cross-link density in the shell was modified. Since both PNIPAM and PNIPMAM are thermosensitive polymers, a general size decrease with temperature is observed. However, the characteristic swelling behavior depends on the thickness and the cross-link density of the shell as will be shown below.

Figure 1 shows the temperature-dependent hydrodynamic radius R_h of four core−shell microgels with different shell thickness of 14, 19, 28, and 41 nm as well as of the PNIPAM core. The cross-linker content of the shell was 9.0 mol % BIS.

Two features are noticed. (i) The particle size increased with increased amount of PNIPMAM shell in both the collapsed and swollen state. Taking into account that the syntheses were performed at 70 °C, where the PNIPAM core is collapsed, we find a linear growth of shell volume with the amount of shell monomer present during synthesis. (ii) The temperature sensitivity strongly depends on the thickness of the PNIPMAM shell. Samples CS005 and CS009 that have a low PNIPMAM content show two regions. Up to 35 °C they display a sharp decrease in particle size corresponding to the PNIPAM core collapse. A less pronounced decrease at temperatures to 45 °C indicates the PNIPMAM shell collapse. At high PNIPMAM (CS008) content, i.e., with a thick shell, the first transition is no longer observed, and the core−shell particle behaves similarly to a pure PNIPMAM microgel.

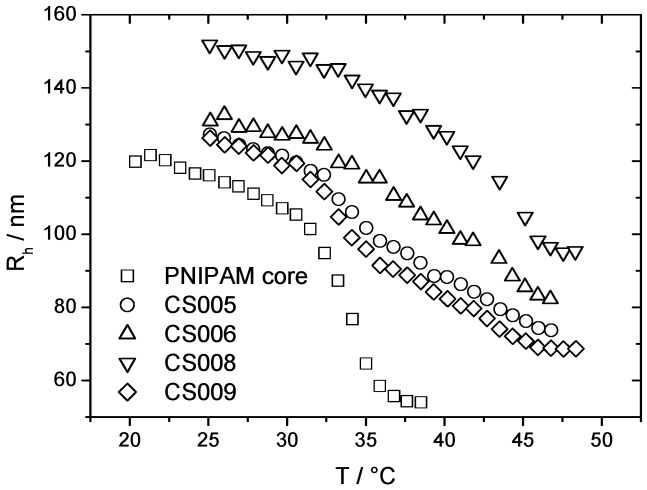

Figure 1. Hydrodynamic radius vs temperature of core−shell microgels with different shell thickness at a shell cross-linker content of 9.0 mol %. The parent PNIPAM core is shown for comparison.

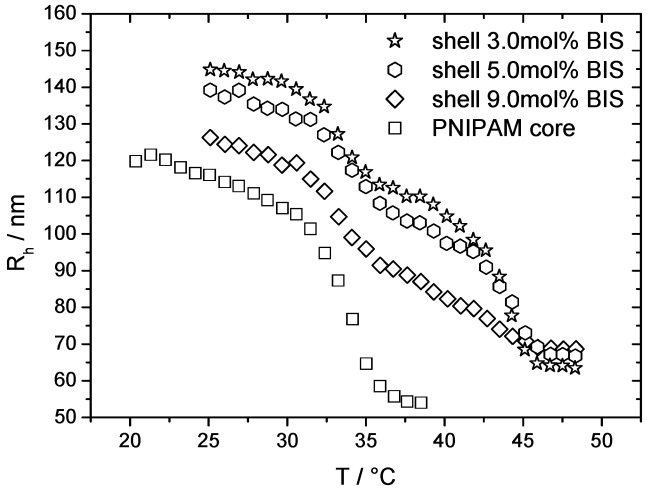

Figure 2. Hydrodynamic radius vs temperature of core−shell microgels with different shell cross-linker content. The parent PNIPAM core is included again.

Similar behavior was observed when the cross-link density in the PNIPMAM shell was varied. Cross-linker contents of 3.0, 5.0, and 9.0 mol % were employed. Figure 2 demonstrates the influence of the shell cross-linker content on the core−shell particles swelling behavior. Sample CS009 with 9.0 mol % cross-linker was already shown in Figure 1. Shell thicknesses at 47 °C are between 9 and 15 nm.

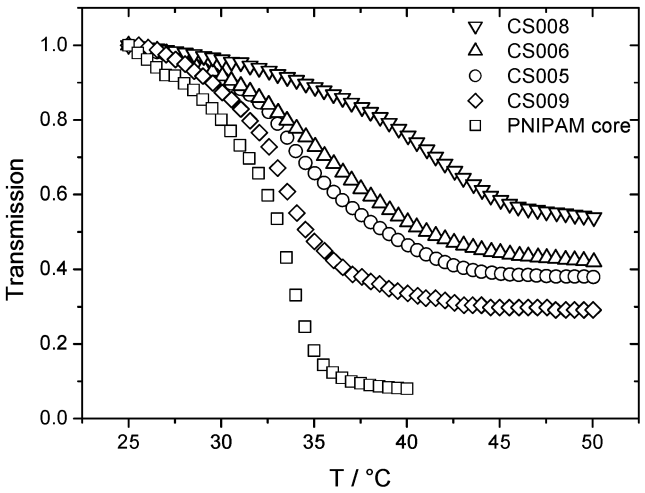

Figure 3. Optical transmission data of core−shell microgels with varying shell thickness and PNIPAM core.

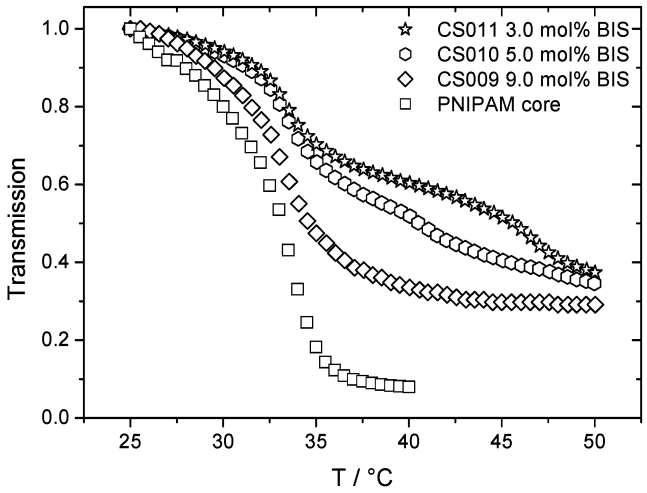

Figure 4. Transmission data of core−shell microgels with shell cross-linker content varied from 3.0 to 9.0 mol %.

These samples reveal two transitions with a pronounced intermediate plateau. The particle size in the totally collapsed state at 48 °C is nearly identical for the three samples. The particles swell with decreasing temperature, and lower shell cross-link density leads to larger hydrodynamic radii. Differential scanning calorimetry (DSC) measurements of these samples show two distinct signals at the LCSTs of PNIPAM and PNIPMAM. In contrast, the sample with a thick and highly cross-linked shell, CS008, revealed no DSC signal at the PNIPAM LCST.

Optical transmission measurements were carried out complementary to dynamic light scattering in order to characterize the samples at concentrations of ca. 0.5 wt %. Figure 3 shows transmission data of core−shell microgels with different shell thickness.

The optical transmission of the core−shell systems at 25 °C increased with increasing shell thickness. In Figure 3 the relative optical transmission is shown; thus, the relative change in transmission was smaller with increasing shell thickness.

The general trend is very similar to what was found in DLS for highly diluted samples. The behavior changes from PNIPAM-like to PNIPMAM-like with increasing shell thickness. However, a smooth transition is observed in all cases, whereas the hydrodynamic radius revealed a two-step process for the same samples (see Figure 1).

In Figure 4, transmission data for core−shell microgels with varied shell cross-linker contents are shown. The two-step process is now observable with the samples that have cross-link density of 3.0 and 5.0 mol %.

Discussion

The results clearly show that the swelling behavior of thermosensitive core−shell microgels can be controlled by mass and cross-link density of the PNIPMAM shell.

A swelling ratio $\alpha = (R_h(T)/R_{h,T>48°C})^3$ can be defined where the temperature-dependent particle size is normalized by the value above 48 °C, i.e., in the collapsed state. Figures 5 and 6 show the swelling ratios for the two series of varied shell thickness and varied shell cross-linker content, respectively.

Significant differences between the samples shown in Figure 5 are found only at temperatures below the core LCST, i.e., in the good solvent limit, when both the shell

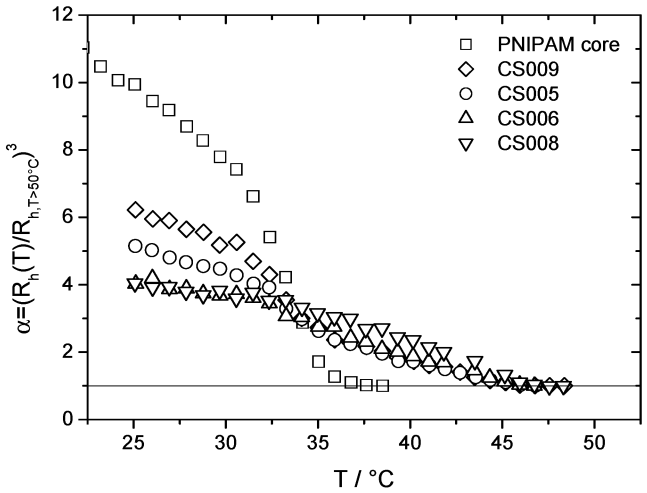

Figure 5. Temperature-dependent swelling ratios α of core−shell microgels with different shell thickness. The PNIPAM core is shown for comparison.

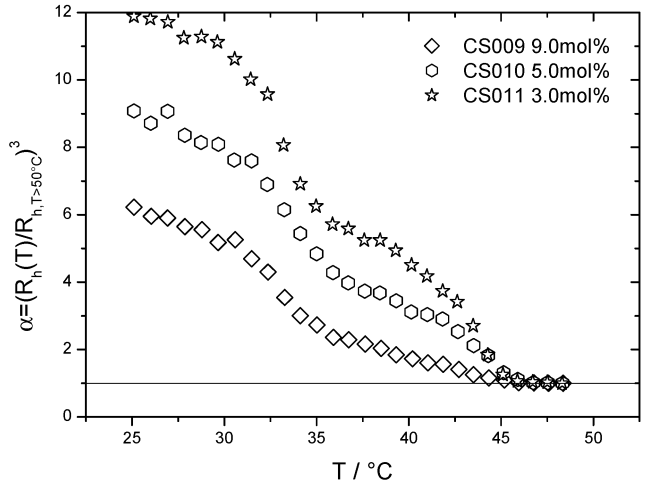

Figure 6. Swelling ratios α of core−shell microgels with varied shell cross-link density.

and core are strongly swollen. A smaller shell thickness leads to a higher swelling ratios of the entire particle. However, at temperatures above the core LCST but below the shell LCST, i.e., 34−44 °C, differences are hardly observed. A series of pure PNIPMAM microgels were prepared with same cross-link densities as were

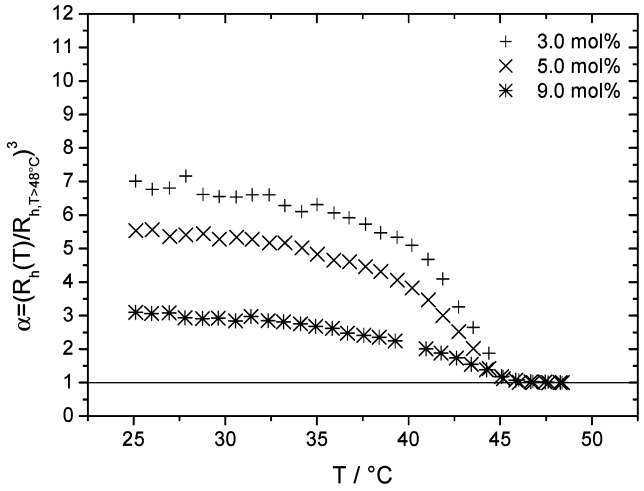

Figure 7. Swelling ratios of pure PNIPMAM microgels with same cross-link densities as employed in core−shell particles.

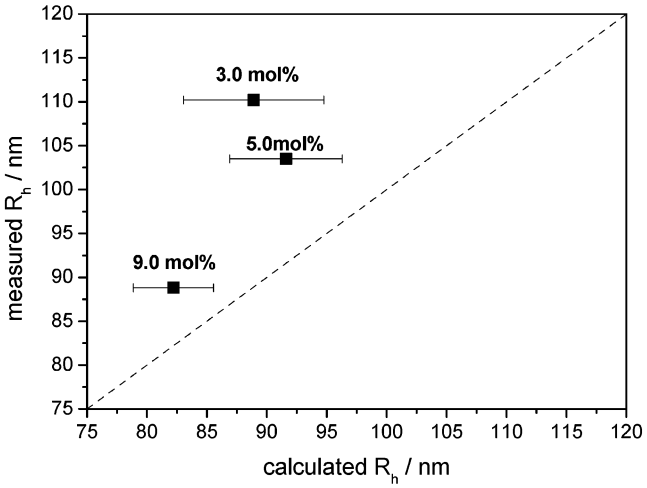

Figure 8. Comparison of calculated and measured particle sizes of core−shell microgels at 37.5 °C with different shell cross-link densities.

applied in core−shell particles and investigated for a quantitative comparison with PNIPAM core and core−shell microgels. Figure 7 shows swelling ratios of pure PNIPMAM microgels with 3.0, 5.0, and 9.0 mol % cross-linker content.

Swelling ratios of 3−7 at 25 °C are found for pure PNIPMAM microgels. The swelling ratio increases with decreased cross-link density as is known for PNIPAM microgels.[17] However, pure PNIPMAM particles swell less as compared to pure PNIPAM particles at the same cross-linker content.[18] Comparing the swelling ratios of core−shell particles with different shell thickness with the 9.0 mol % cross-linked PNIPMAM and the parent PNIPAM core at 25 °C, we find values between these boundaries. The swelling ratio is bigger than the swelling ratio of a pure PNIPMAM microgel with same cross-linker content, even for particles with a thick shell, i.e., CS008. This effect is due to the core contribution to the entire particle volume. When the shell thickness is decreased, the swelling ratios at temperatures below 34 °C increase. A growing influence of the core to the particles swelling behavior is observed; below 34 °C the expanding core presses the shell outward. But this expansion is limited by a mechanical stress in the shell. So the swelling ratio of the parent pure PNIPAM cannot be reached. The balance between expansion of the core and mechanical stress in the shell is an effect of the shell thickness. When a specific shell thickness is exceeded, the influence of the core is not longer observable.

Figure 6 shows swelling ratios of core−shell microgels that have different shell cross-link densities, and the expected behavior is found. At temperatures between 34 and 44 °C the shell swells depending on the cross-link density. Below 34 °C the core swells and presses the shell outward.

For a more detailed discussion we will employ a simple model to calculate a particle size at 37.5 °C (where the intermediate plateau is found) from particle sizes at 48 °C and the known swelling ratios of the shell. Synthesis was performed at 70 °C where water is a poor solvent for both PNIPAM and PNIPMAM. Hence, the collapsed state should be taken as the reference state for the particles (index 0). The difference of the particle sizes at a temperature above the shell LCST is $R^0_{CS} - R^0_C = \Delta R$, where R^0_{CS} and R^0_C are the radii of core−shell microgel and core, respectively, in the reference state. From ΔR we can calculate the shell volume V^0_S in the collapsed state. A shell volume for any temperature between 34 and 44 °C can now be calculated by multiplying the shell volume V^0_S by the swelling ratio $\alpha(T)$ of a pure PNIPMAM microgel with the same cross-link density: $V_S(T) = \alpha(T)V^0_S$. The particle radius can be calculated from the sum of core and shell volume: $R_h(T) = [3(V^0_C + V_S(T))/4\pi]^{1/3}$, and the results are shown in Figure 8.

In all cases the measured particle size is found to be larger than the calculated radius. That demonstrates that both core and shell do not swell independently but influence each other.

Ballauf and co-workers have investigated core−shell particles with a rigid sphere polystyrene core and a thermosensitive PNIPAM shell.[19] Using SANS and SAXS techniques, they could show that the swelling process is restricted due to the fixation of the network on the polystyrene surface. The network can only expand along the surface normal direction. Swelling in the two other directions is limited by spatial constraint. In our samples the shell is attached to a swellable network. We explain the bigger experimental radius that the shell avoids the constraint by widening the shell sphere. The core is collapsed, but since it is only lightly cross-linked, the forces which would restrain the shell are weak. Thus, the shell will mechanically expand the collapsed core. One could suspect that the core in those samples which have a thick PNIPMAM shell is almost fully expanded at temperatures above the PNIPAM LCST.

Preliminary small-angle neutron scattering measurements on sample CS010 were performed at D11 instrument at the ILL, Grenoble. The concentration was 0.2 wt % in D_2O. In Figure 9 SANS data for three different temperatures are shown. The sample was investigated at a temperature where both core and shell are swollen (32 °C), a temperature where the core is expected to be collapsed (39 °C), and a temperature where both core and shell are collapsed (50 °C).

At 32 °C, the scattering intensity at high q is found to be proportional to the scattering vector $q = |\vec{q}| = 4\pi/\lambda \sin(\Theta/2)$ with $I(q) \propto q^{-1}$;[33] almost the same scattering exponent was found for pure PNIPAM microgels by Kratz et al.[20] When the temperature is increased to 39 °C, a particle form factor with a minimum at ∼0.009

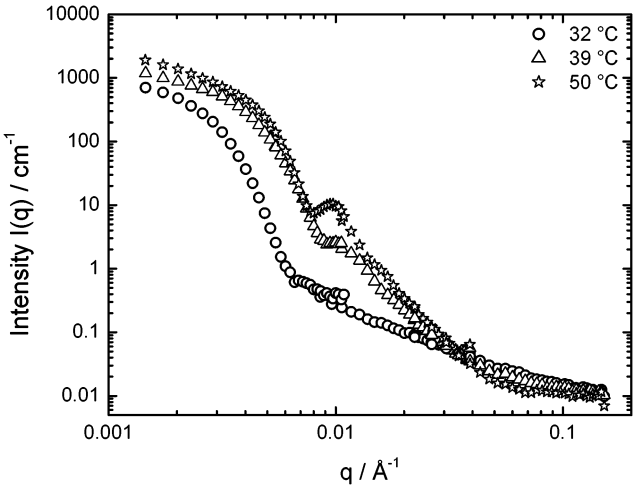

Figure 9. Small-angle neutron scattering spectra of sample CS010 below core LCST (T = 32 °C), between core and shell LCST (T = 39 °C), and above shell LCST (T = 50 °C). The form factor minimum shifts toward lower q with increasing temperature.

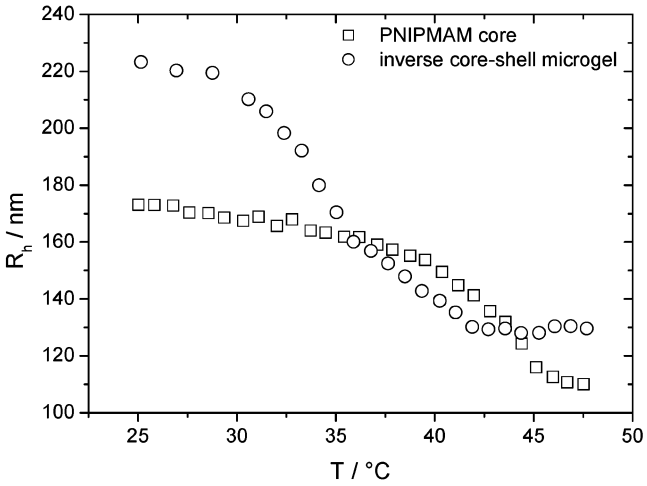

Figure 10. Hydrodynamic radii vs temperature of inverse core−shell microgel and parent PNIPMAM microgel.

Å^{-1} is observable, and the scattering exponent at high q is −3.2. For T = 50 °C Porod scattering with $I(q) \propto q^{-4.1}$ is found in the same manner as for pure PNIPAM microgels,[21,22] which is characteristic for scattering of a phase-separated structure with sharp interfaces. However, the form factor minimum shifts to lower q values with increasing temperature, which at first sight suggests an increasing particle size. However, the slope at low q decreases with increasing temperature, indicating a decreasing radius of gyration, which is in agreement with the DLS data that unambiguously revealed that the hydrodynamic radius decreases with temperature. At 39 °C $I(q) \propto q^{-3.2}$ is observed in the high q regime, and one can suppose that scattering is dominated by a partially collapsed core. This suggests that the intensity minimum characterizes the core. At 50 °C the shell collapses as well, and the apparent particle size increases as scattering occurs on the shell surface. So the minimum will shift toward lower q. This model suggests strong differences of local segment density in core and shell, respectively, at different temperatures. Thus, a direct modeling of the SANS data should provide detailed information on segment densities and therefore on the temperature-dependent swelling of core and shell. Such data analysis is in progress and will be presented elsewhere.[23]

Finally, an inverse core−shell microgel (sample INV001) with a PNIPMAM core (7.0 mol % cross-linker) and a PNIPAM shell (5.0 mol % cross-linker) was prepared and investigated by DLS; Figure 10 shows the temperature-dependent hydrodynamic radius.

The inverses system displays interesting features. In the collapsed state (where synthesis was performed) the radius of the inverse core−shell microgel is 19 nm bigger as compared to the PNIPMAM core. At intermediate temperatures of 34−44 °C, however, the hydrodynamic radius of the core−shell system is smaller than that of the core. Obviously, the collapsed PNIPAM shell strongly restricts the swelling of the PNIPMAM core, so that the core cannot expand to its native volume. This results in an overall particle size that is smaller as compared to the parent core. Below the PNIPAM LCST, both core and shell swell, and the core−shell system has again a larger radius as compared to the core. This behavior is in good agreement with what was discussed above concerning the PNIPAM core−PNIPMAM shell systems and nicely demonstrates the mutual influencing of core and shell swelling.

Conclusions

Doubly thermosensitive core−shell microgels consisting of an PMIPAM core and a PNIPMAM shell have been prepared and investigated by dynamic light scattering, optical transmission, and small-angle neutron scattering. An inverse core−shell microgel where the core shrinks at higher temperatures than the shell was prepared as well. The results demonstrate that shell thickness and cross-link density of the shell control the thermosensitive behavior of the entire particle and that core and shell influence each other. With the inverse system, the collapsed shell at intermediate temperatures strongly restricts the core swelling so that the overall size of the core−shell microgel is smaller as compared to the pure core. Thus, it is possible to have a rational synthesis of thermosensitive microgels that display one or two distinct volume transitions as a function of temperature. SANS data reveal interesting information on segment densities at different temperatures.

PNIPAM−PNIPMAM particles are colloidally stable in concentrated solution until the PNIPMAM LCST is reached. The inverse system becomes colloidally unstable above the PNIPAM LCST as is known from core−shell particles with a rigid core. However, the thermosensitivity of the PNIPMAM core in the core−shell microgel allows to alter the structure even in the flocculated state, which will provide for example interesting aging phenomena. This will be explored in the future.

Acknowledgment. Financial support by the Deutsche Forschungsgemeinschaft (DFG) and the Fonds der Chemischen Industrie is gratefully acknowledged. We thank the ILL, Grenoble, France, and especially P. Lindner for beam time at the D11 instrument.

References and Notes

(1) Chen, S.; Hoffman, A. S. *Macromol. Rapid Commun.* **1995**, *16*, 175.
(2) Bergbreiter, D. E.; Case, B. L.; Liu, Y. S.; Caraway, C. W. *Macromolecules* **1998**, *31*, 6053.
(3) Pelton, R. H.; Chibante, P. *Colloids Surf.* **1986**, *20*, 247.

(4) Saunders, B. R.; Vincent, B. *Adv. Colloid Interface Sci.* **1999**, *80*, 1.
(5) Pelton, R. *Adv. Colloids Interfaces* **2000**, *85*, 1.
(6) Senff, H.; Richtering, W. *J. Chem. Phys.* **1999**, *111*, 1705.
(7) Senff, H.; Richtering, W. *Colloid Polym. Sci.* **2000**, *278*, 830.
(8) Zhou, S.; Chu, B. *J. Phys. Chem. B* **1998**, *102*, 1364.
(9) Zha, L.; Hu, J.; Wang, C.; Fu, S.; Elaissari, A.; Zhang, Y. *Colloid Polym. Sci.* **2002**, *280*, 1.
(10) Mielke, M.; Zimehl, R. *Ber. Bunsen-Ges. Phys. Chem.* **1998**, *102*, 1698.
(11) Daly, E.; Saunders, B. R. *Langmuir* **2000**, *16*, 5546.
(12) Jones, C. D.; Lyon, L. A. *Macromolecules* **2000**, *33*, 8301.
(13) Gan, D.; Lyon, L. A. *J. Am. Chem. Soc.* **2001**, *123*, 7511.
(14) Jones, C. D.; Lyon, L. A. *Langmuir* **2003**, *19*, 4544.
(15) Duracher, D.; Elaissari, A.; Pichot, *J. Polym. Sci., Part A* **1999**, *37*, 1823.
(16) Duracher, D.; Elaissari, A.; Pichot, C. *Colloid Polym. Sci.* **1999**, *277*, 905.
(17) Wu, X.; Pelton, R. H.; Hamilelec, A. E.; Woods, D. R.; McPhee, W. *Colloid Polym. Sci.* **1994**, *272*, 467.
(18) Duracher, D.; Elaissari, A.; Pichot, C. *Macromol. Symp.* **2000**, *150*, 305.
(19) Seelenmeyer, S.; Deike, I.; Rosenfeldt, S.; Norhausen, C.; Dingenouts, N.; Ballauf, M.; Narayanan, T.; Lindner, P. *J. Chem. Phys.* **2001**, *114*, 10471.
(20) Kratz, K.; Hellweg, T.; Eimer, W. *Ber. Bunsen-Ges. Phys. Chem.* **1998**, *102*, 1603.
(21) Kratz, K.; Hellweg, T.; Eimer, W. *Polymer* **2001**, *42*, 6631.
(22) Crowther, H. M.; Saunders, B. R.; Mears, S. J.; Cosgrove, T.; Vincent, B.; King, S. M.; Yu, G. E. *Colloids Surf. A* **1999**, *152*, 237.
(23) Berndt, I.; Lindner, P.; Pedersen, J. S.; Richtering, W., manuscript in preparation.

MA034771+